Investigation of composites under compression at ISD
Past, Present and Future

ICCM23

31 July – 04 August 2023, Belfast, Northern Ireland

by

Nabeel Safdar and Prof. Raimund Rolfes
Institute of Structural Analysis, Leibniz University Hannover, Germany

Email: n.safdar@isd.uni-hannover.de, r.rolfes@isd.uni-hannover.de

Contents

- Introduction
- Approaches
  - Mechanics of failure and post failure response
  - Quantification of uncertainty in strength
- Outlook

Introduction

INSTITUT FÜR STATIK UND DYNAMIK

Importance

- Increasing importance of light weight structures
- Fiber Reinforced Polymers (FRPs) offer excellent strength to weight ratios

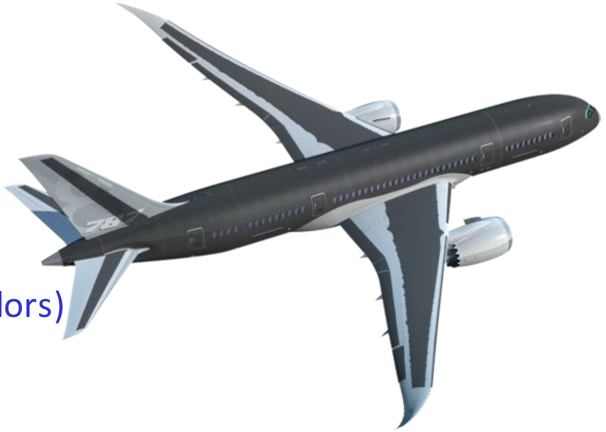

Fiber reinforced polymers (dark colors) in Boeing 787 Dreamliner

A design limiting failure mode

- Strength under predominant compression limited by ***Microbuckling*** (MB)
- Shear localization leading to final fracture
- Highly sensitive to manufacturing induced initial fiber misalignments
- Fiber misalignments lead to scatter in strength in predominant compression loads

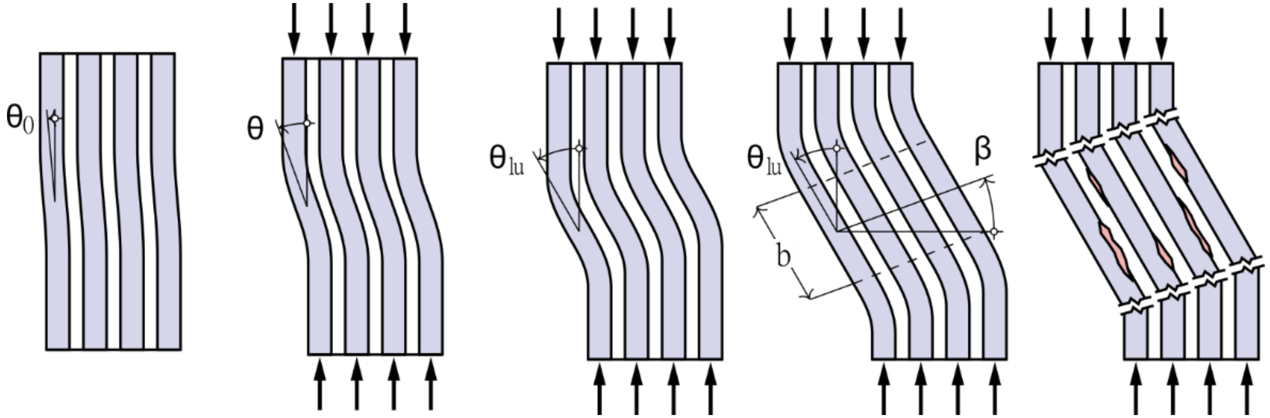

Microbuckling failure schematic

Approaches

Mechanics of failure and post failure response

- Micro modeling
- Homogenized modeling (Micropolar continuum, Conventional continuum)

Quantification of uncertainty in strength

- Experimental determination of failure probability
- Numerical modeling for failure probability

Mechanics of failure and post failure response

Micro modeling

- Ref [1]: Epoxy modeled as elasto-plastic material with quadratic yield surface *f* and damage initiation *d* dependent on hydrostatic pressure *p*

$$f = \sigma_{VM}^2 - a_0 - a_1 p \qquad d = \sigma_{VM}^2 - b_0 - b_1 p$$

- Orthotropic material model with Hashin failure criteria for fibers.
- Material imperfection in form of idealized sinusoidal misalignment
- Kink band angle, effect of local and global misalignment, and different aspects of kink band formation analyzed

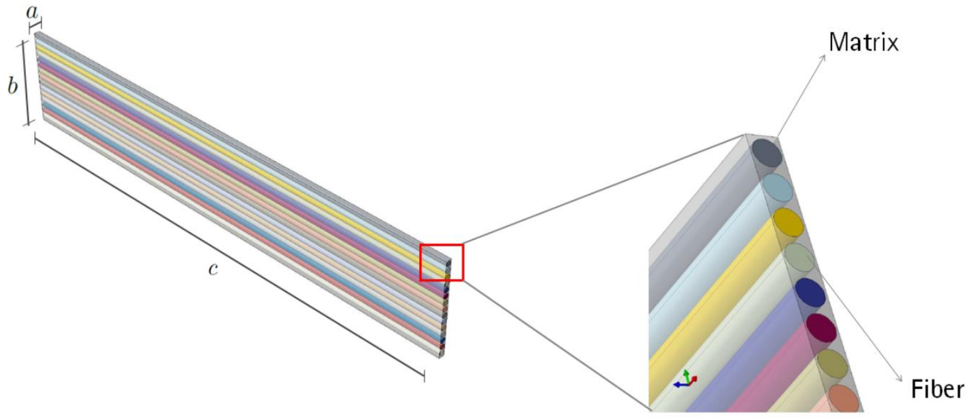

Micro model of UD layer

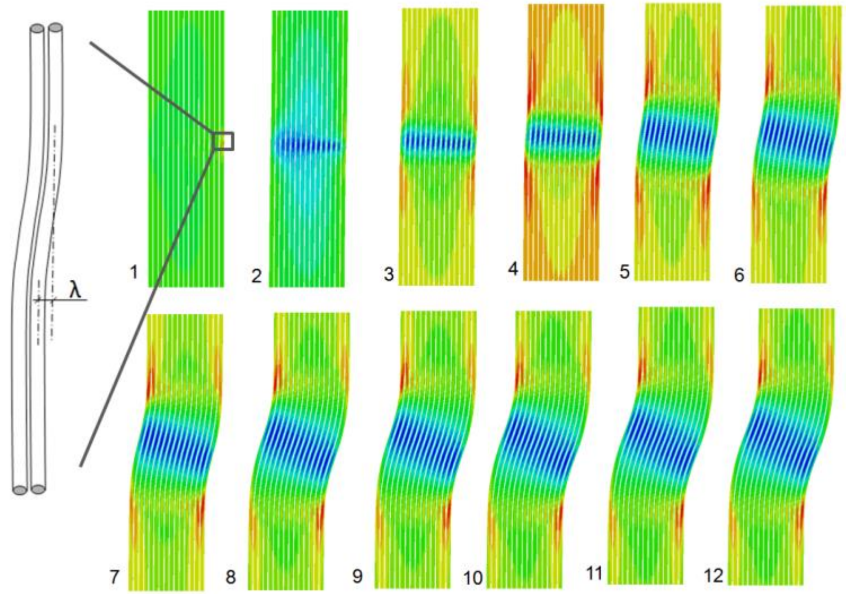

Different stages in formation of a kink band

Mechanics of failure and post failure response

Hybrid micro meso modeling

- Ref [2]: 0-deg plies modeled as micro, off-axis plies modeled as meso
- Transversely isotropic elastic-plastic material model with following yield surface

$$F(\sigma, \bar{\varepsilon}^p, \mathbf{A}) = \alpha_1 I_1 + \alpha_2 I_2 + \alpha_3 I_3 + \alpha_{32} I_3^2 - 1$$

- Interactions between fiber kinking, matrix cracking and delamination analyzed

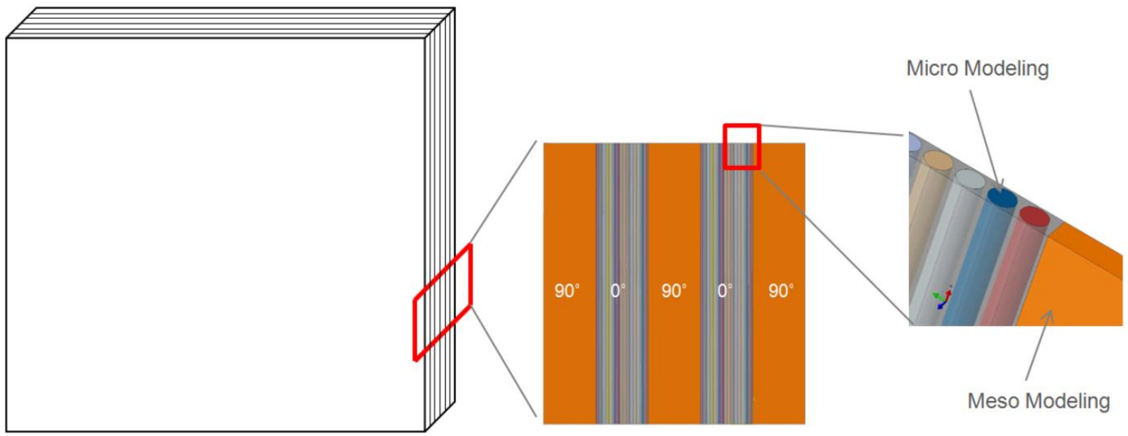

Hybrid micro meso model of a multidirectional laminate

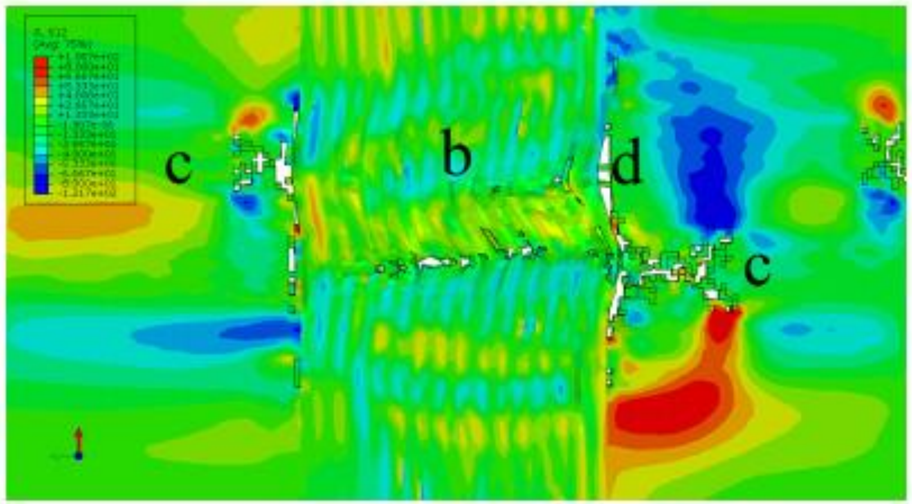

Different mechanisms in 90-0-90-0-90 ply model

b:kink band, c: matrix cracking, d: delamination

Mechanics of failure and post failure response

Homogenized modeling (Micropolar continuum)

- Ref[3]: Additional rotational degrees of freedom to account for curvature strain
- Implemented in 2D adapting finite strain plasticity
- Major benefit in post peak response

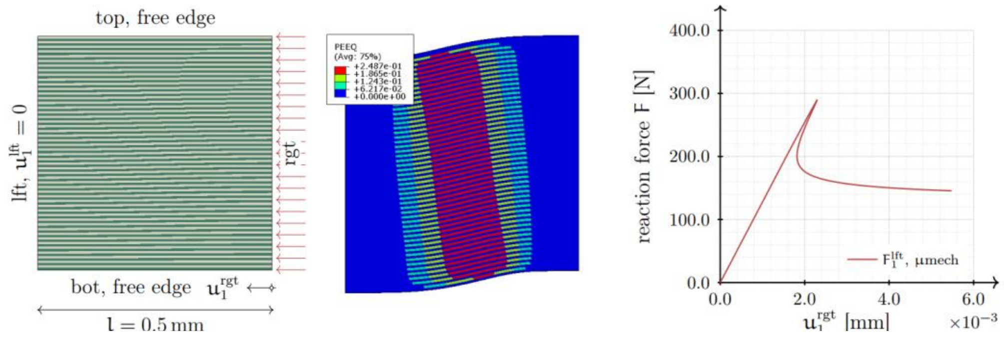

Reference micromechanical model:

(a) Undeformed mesh, (b) mesh at max deformation, (c) F-d diagram

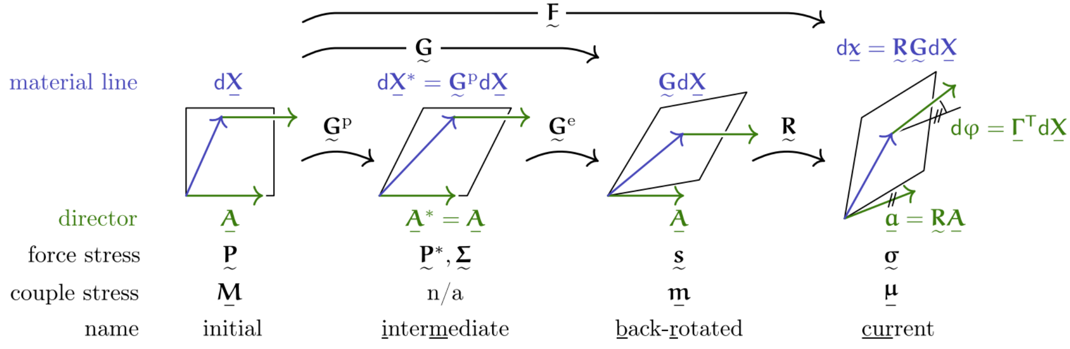

Schematic of the different kinematic and kinetic quantities

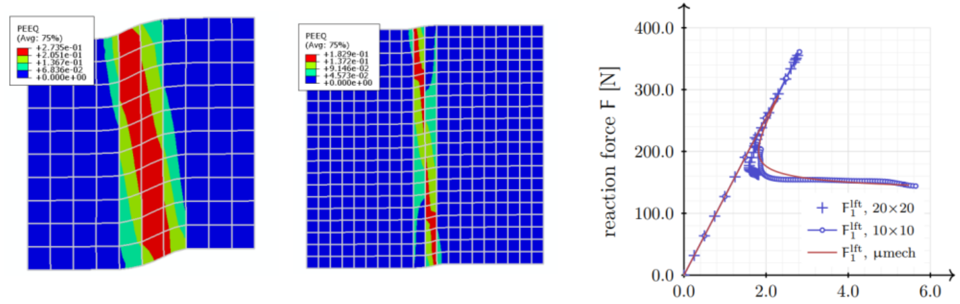

Conventional homogenized model:

At max deformation (a) mesh 10x10, (b) mesh 20x20, (c) F-d diagram

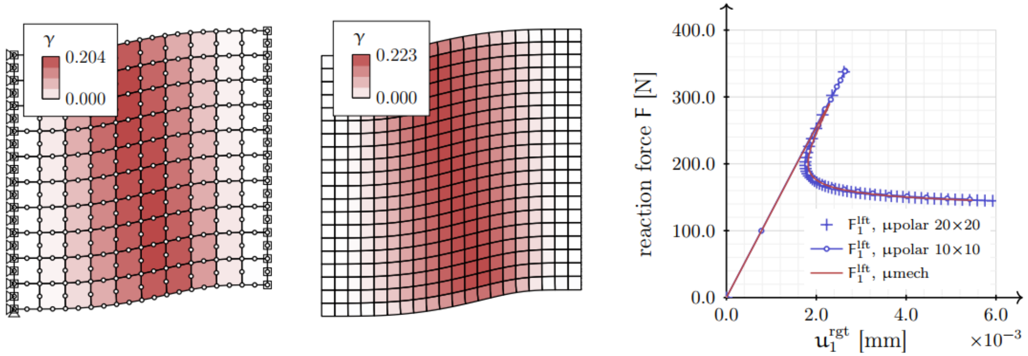

Micropolar homogenized model:

At max deformation (a) mesh 10x10, (b) mesh 20x20, (c) F-d diagram

Mechanics of failure and post failure response

Homogenized modeling (Conventional continuum)

- Ref[4]: Anisotropic pressure dependent yield function with non-associated plastic potential function

$$G(\sigma, \mathbf{A}) = \zeta_1 I_1 + \zeta_2 I_2 + \zeta_3 I_3^2 - 1$$

- Cast into corotational framework to account for geometrical non linearities of large rotations
- Implemented in a Abaqus/Implicit UMAT

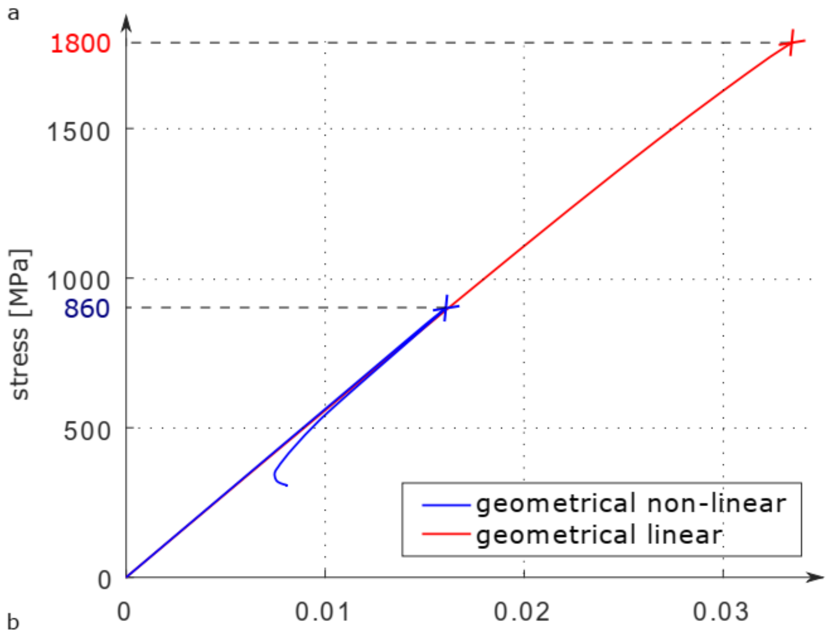

Stress strain response of a 3D homogenized model containing idealized sinusoidal misalignment with and without geometric nonlinearity consideration

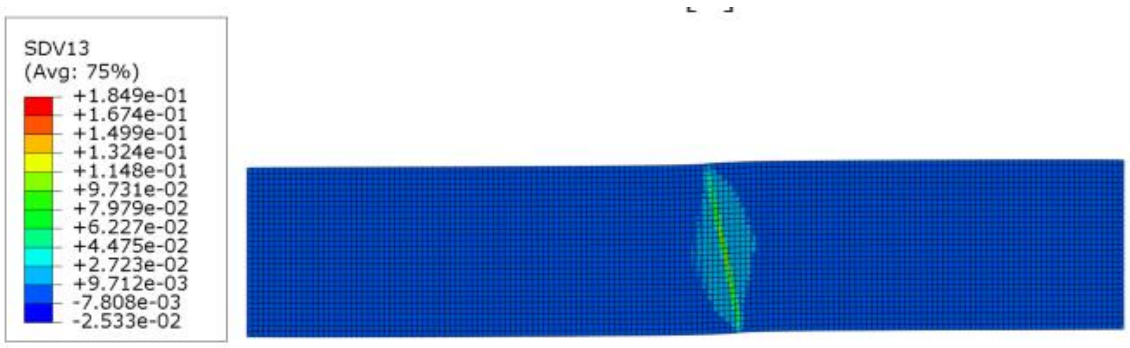

Kink band shown by equivalent plastic strain localization

Mechanics of failure and post failure response

Homogenized modeling (Conventional continuum)

- Ref[5]: Abaqus limitation in homogenized approaches with rotation of preferred direction vector (Wisnom 1993)
- Solution: Rotate the current orientation of preferred direction vector by shear strains
- Verification against Budiansky's analytical formula

$$\boldsymbol{a'} = [1 \quad 0 \quad 0]$$

$$\boldsymbol{b'} = [\cos(\varepsilon^i_{12}) \cdot \cos(-\varepsilon^i_{13}) \quad \cos(-\varepsilon^i_{13}) \cdot \sin(\varepsilon^i_{12}) \quad -\sin(-\varepsilon^i_{13})]$$

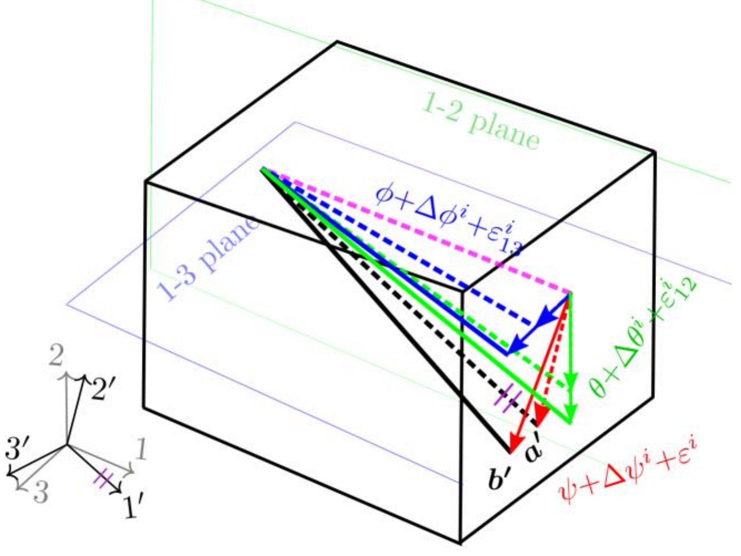

Rotated orientation of preferred direction

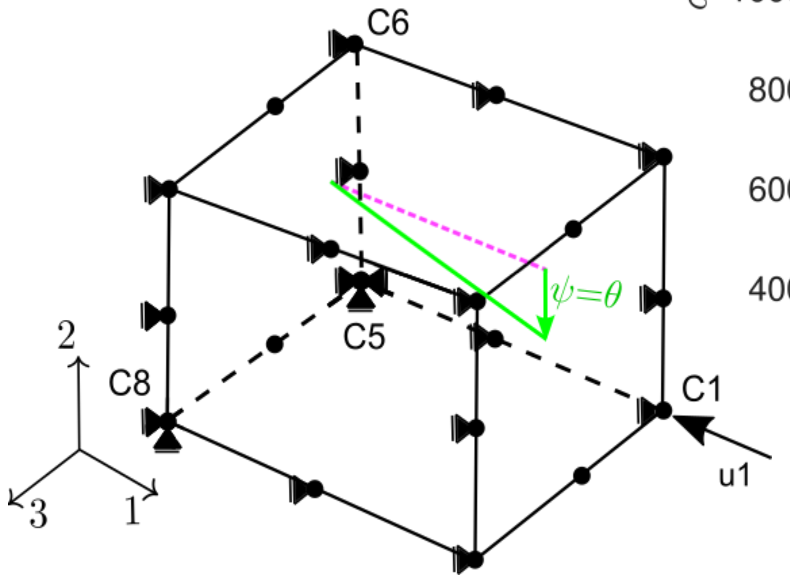

Schematic of 1 element model for verification

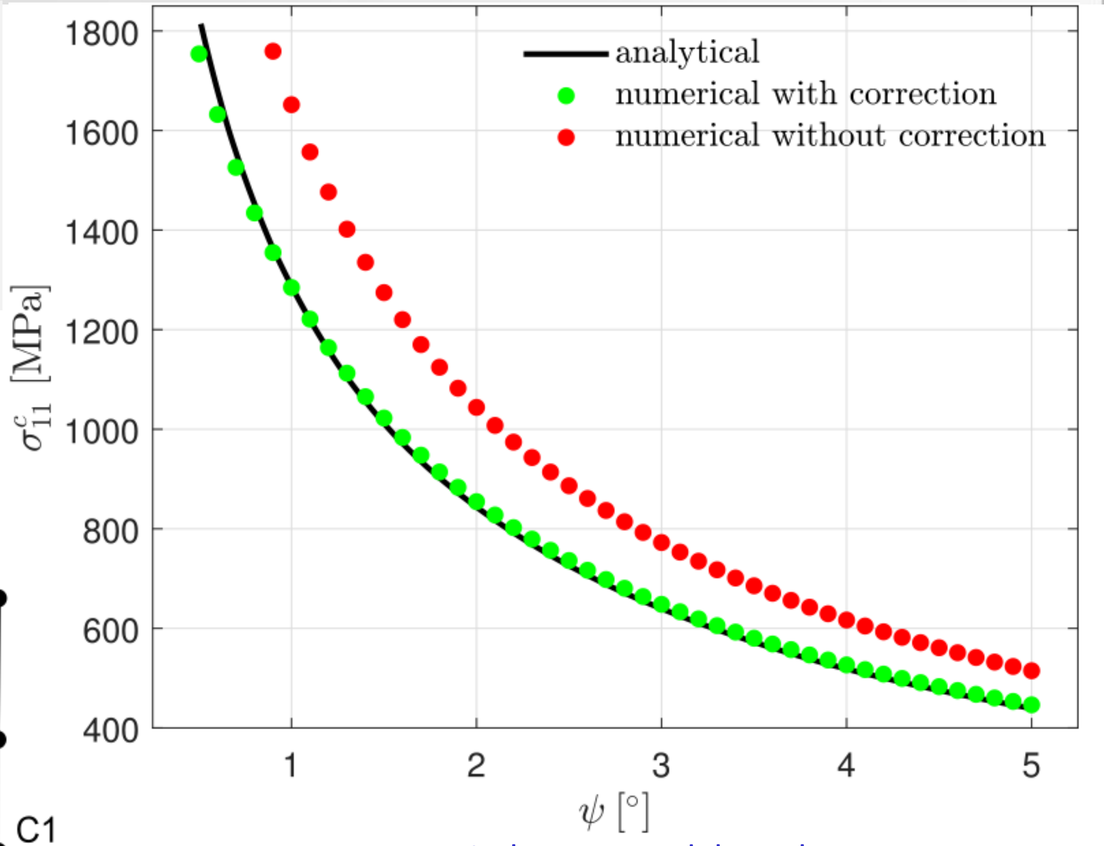

1 element model results

$$\sigma^c_{11} = \max_{\gamma} \left(\frac{\tau_{12}(\gamma)}{\psi + \gamma} \right)$$

Budiansky's analytical solution

Mechanics of failure and post failure response

Homogenized modeling (Conventional continuum)

- [Ref. 6]: Effect of the Misalignment Dimensionality
- 1D and 2D sine waves for 2D modeling, and 2D and 3D sine waves for 3D modeling of the in-plane misalignment angle θ.

$$\max|\theta| = 2.5^\circ$$

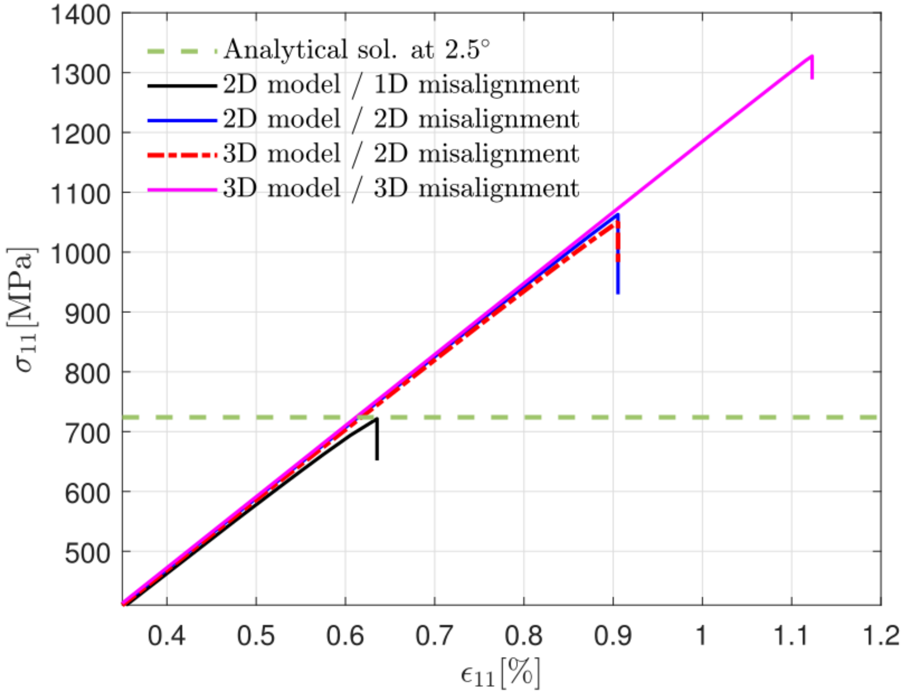

Stress-strain response

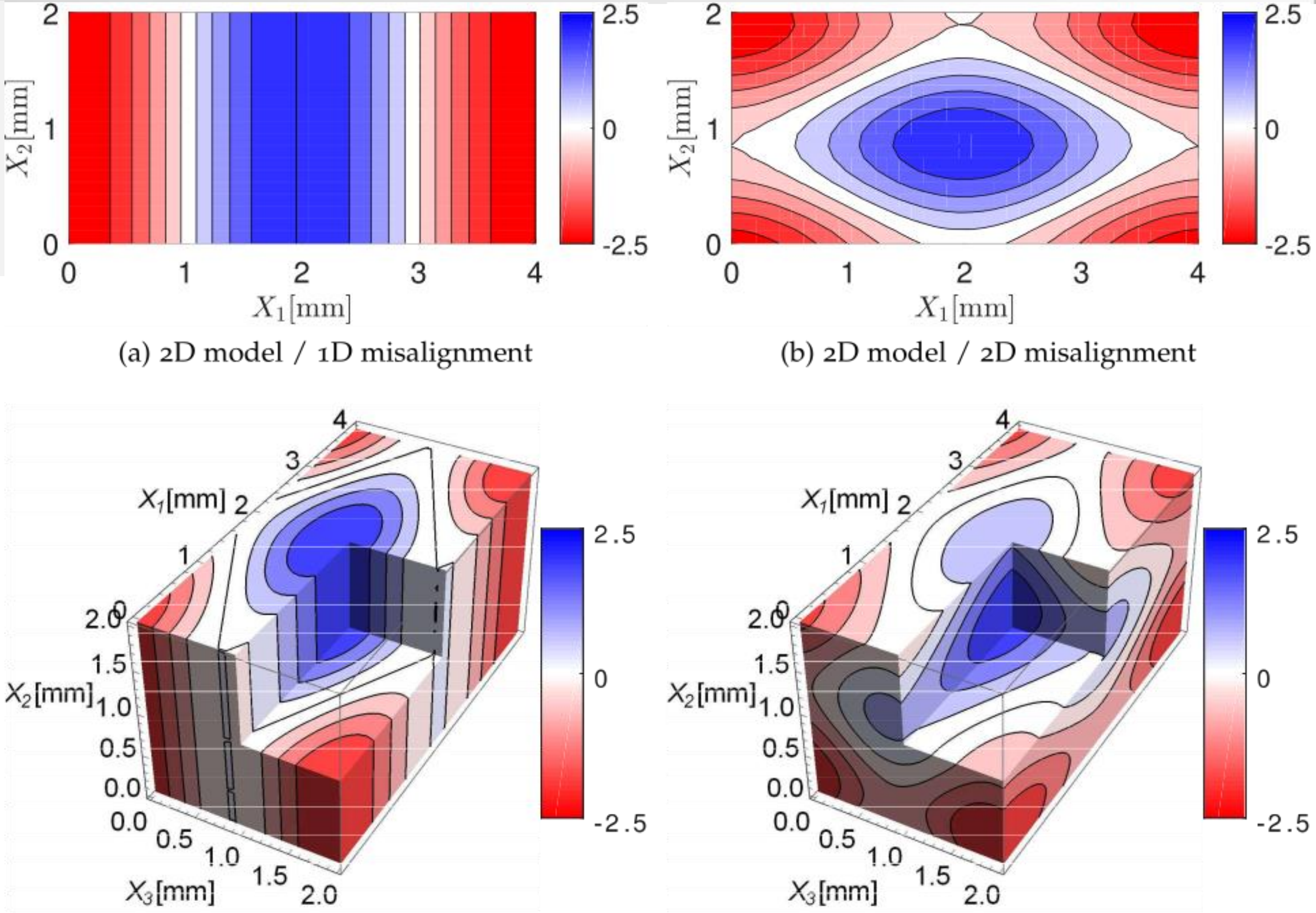

(a) 2D model / 1D misalignment (b) 2D model / 2D misalignment

(c) 3D model / 2D misalignment (d) 3D model / 3D misalignment

Quantification of uncertainty in strength

Experimental determination of failure probability: New fixture design

- [Ref. 7]: Load transfer into the specimen through combined shear and end loading similar to the current standard ASTM-D6641
- Testing under axial compression and combined compression-shear
- Dimensions of specimen gauge section: 5x5x1.15 mm with tabs having tab angle of 45°

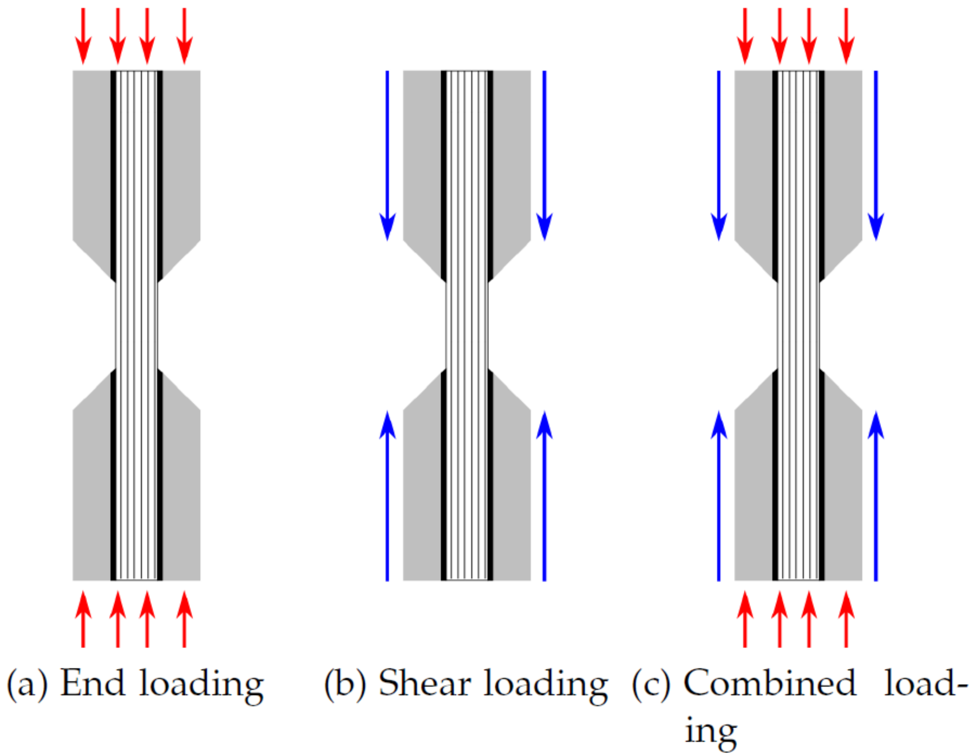

Schematic of load transfer methods

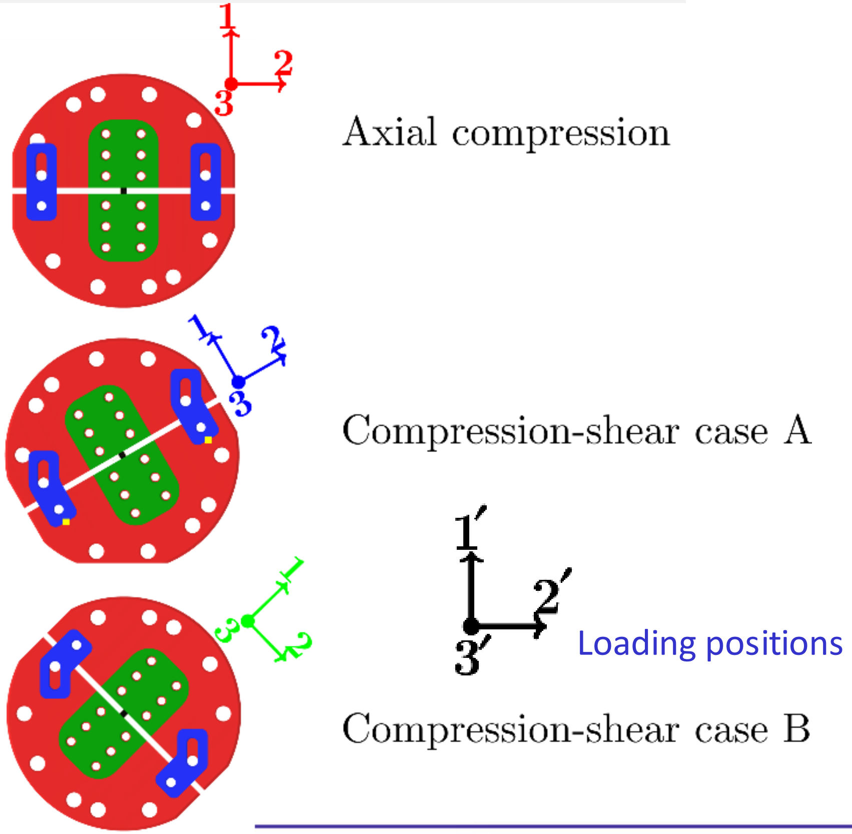

Loading positions

Fixture Design

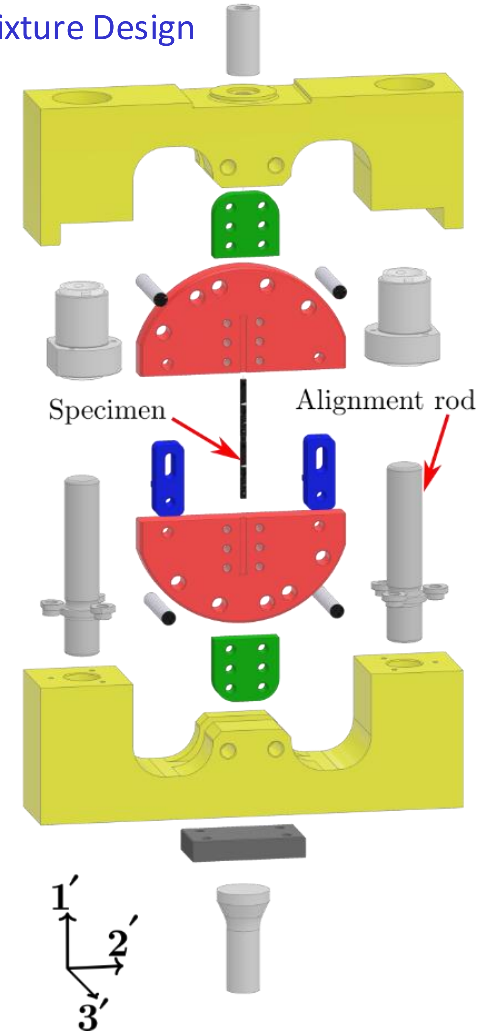

Quantification of uncertainty in strength

Experimental determination of failure probability: Failure mode

- [Ref. 7]: Nominal fiber direction parallel to specimen edges for all load cases
- Microbuckling failure mode observed in all load cases

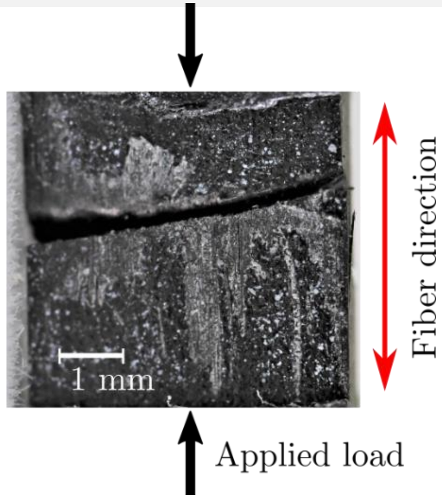

Axial compression

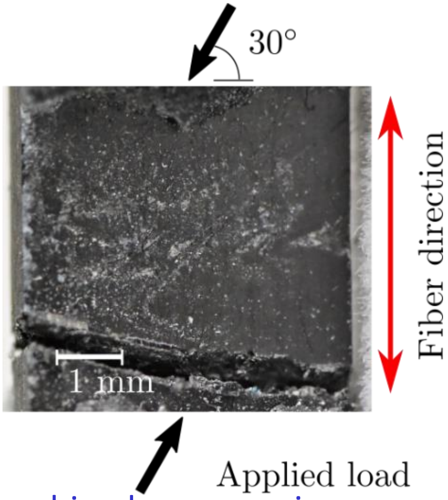

Combined compression-shear case A

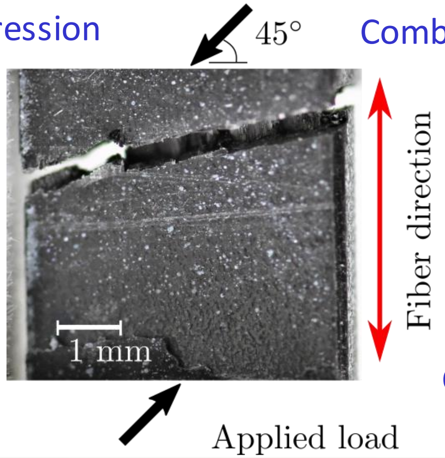

Combined compression-shear case B

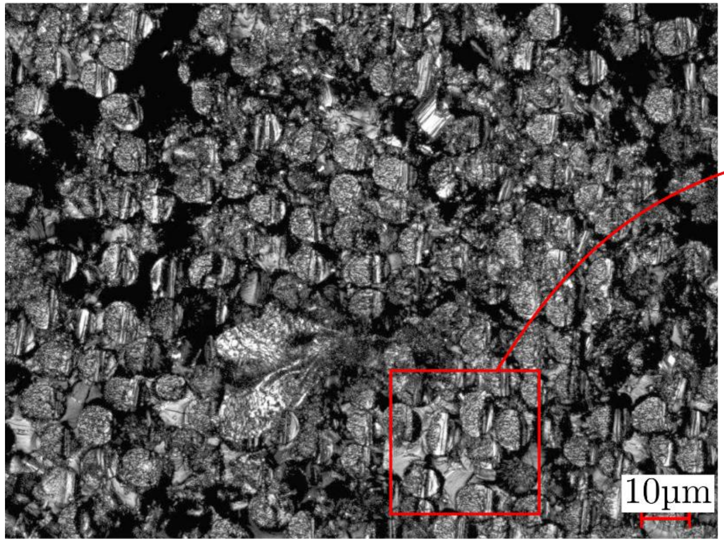

Surface scan of a sample from case B

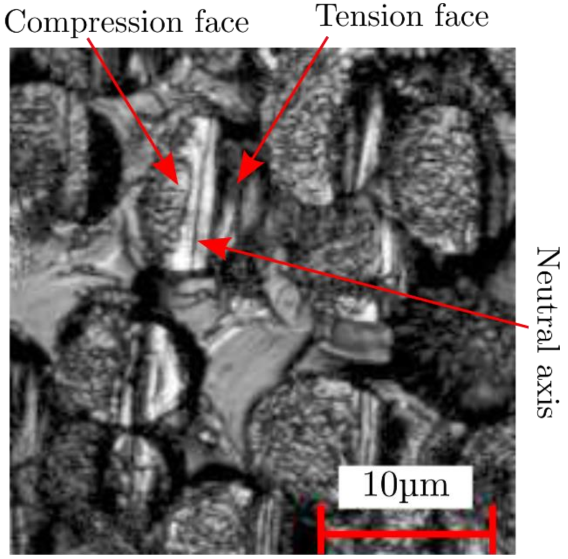

Zoomed in region

Fixture Setup

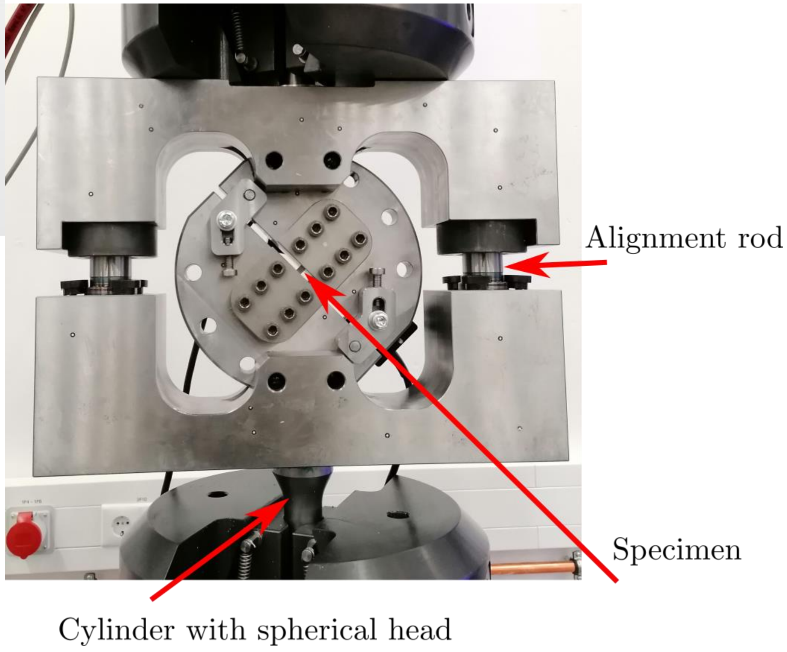

Quantification of uncertainty in strength

Experimental determination of failure probability: Failure Envelope in Strain Space

- [Ref. 7]: 25 successful tests for each load case, survival probability of applied stress given
- Strains measured directly on specimen surfaces using Digital Image Correlation
- Strain envelopes at 25th percentile, median, and 75th percentiles

$$_i(\varepsilon_{11}, \varepsilon_{12}) = p_i \varepsilon_{11} \varepsilon_{12} + q \varepsilon_{12} - r_i \varepsilon_{11} - 1$$

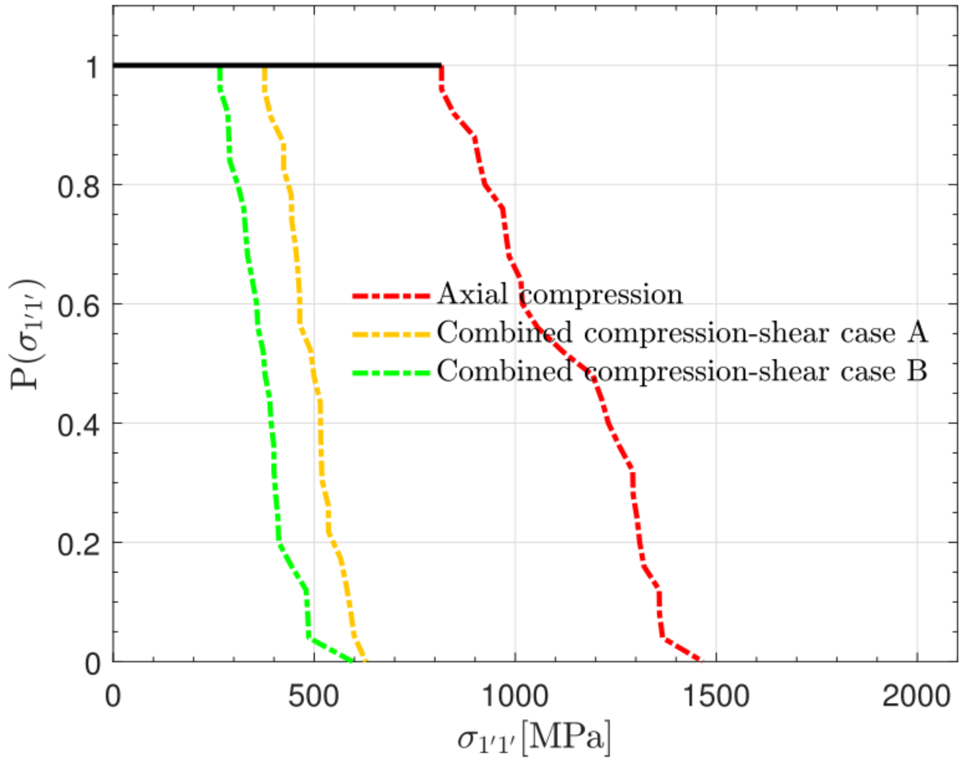

Empirical probability of survival of the applied stress

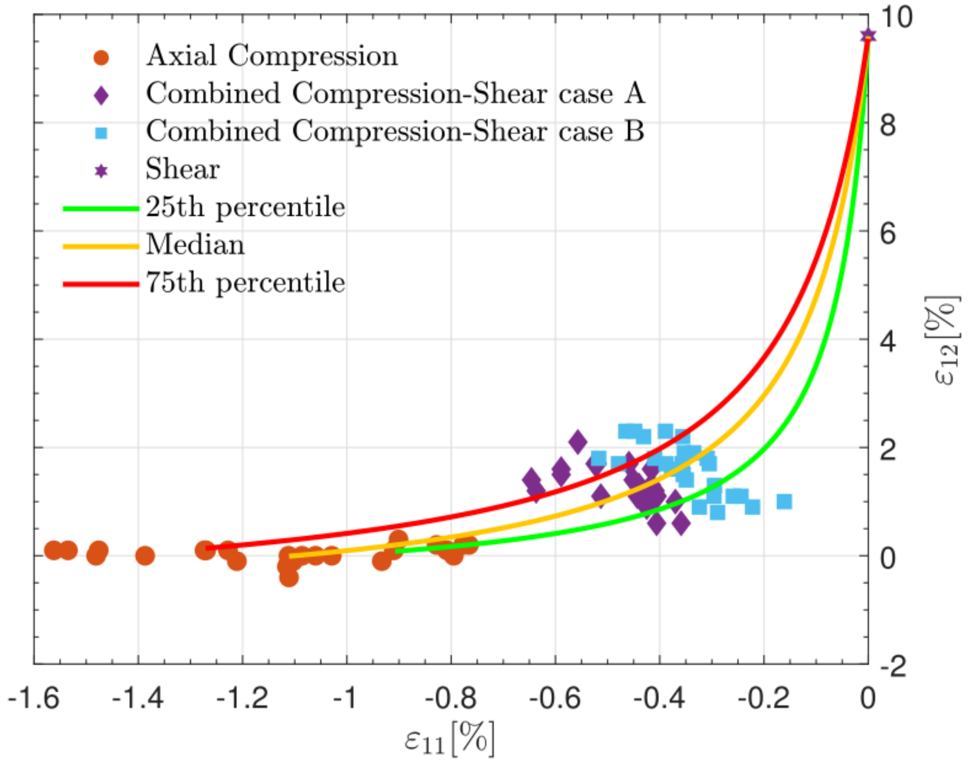

Failure envelope in strain space

Quantification of uncertainty in strength

Experimental determination of failure probability: Failure Envelope in Stress Space

- [Ref. 7]: Applied stresses measured through load cell cannot be divided into components
- Median value of stresses for combined load cases A and B derived using equation system below
- Approx. envelopes at 25th percentile and 75th percentiles

$$g_i(\sigma_{11}, \sigma_{12}) = \frac{\sigma_{11}}{R_{11}^i} + \frac{\sigma_{12}}{R_{12}} - 1$$

$$\sigma_{11}^c = E_{11}\varepsilon_{11}^c$$

$$\sigma_{11}^c = \max_{\gamma_{12}} \left(\frac{\tau(\gamma_{12}) - \sigma_{12}^\infty}{\psi + \gamma_{12} - \gamma_{12}^\infty} \right)$$

$$\gamma \approx \gamma_{12} \qquad \gamma_{13} \approx 0$$

$$\psi = P_{90}(|\Theta_j|) = 1.11^\circ$$

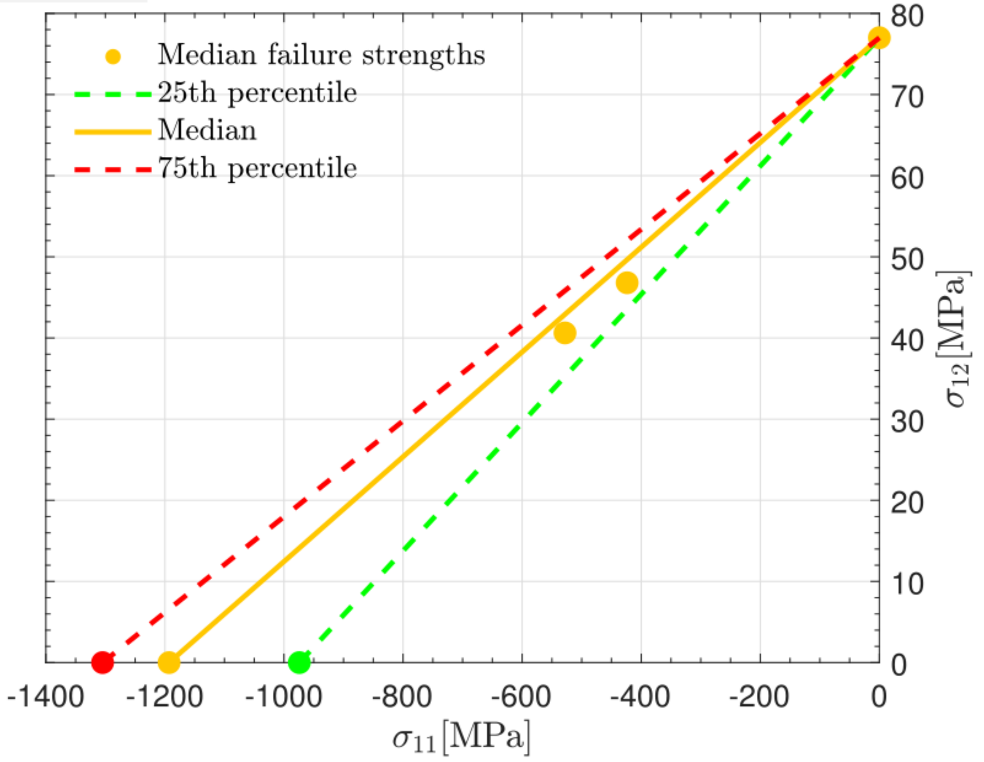

Failure envelope in stress space

- [Ref. 5]: Generated distributions using the calculated spectral densities
- 3 model series generated based on sample 1 (s1), sample 2 (s2), and their average (avg) spectral density characterization
- Characteristics preserved: such as standard deviation and correlation lengths of misalignment angles
- Dimensions: 6.657x1.1412x0.951 mm

$$F_{k,l,m} = \sqrt{\frac{(2\pi)^3}{L_1 L_2 L_3} S_{k,l,m}} \exp\left(\iota \beta_{k,l,m}\right)$$

$$\Xi = \frac{L_1 L_2 L_2}{(2\pi)^3} (s)^2$$

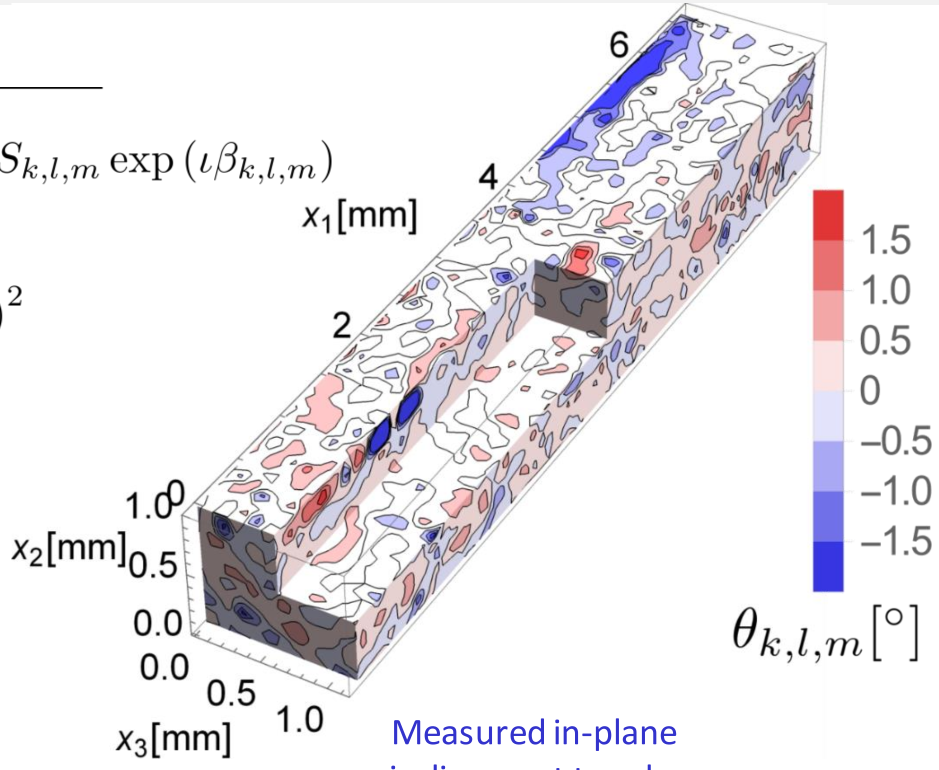

Measured in-plane misalignment topology

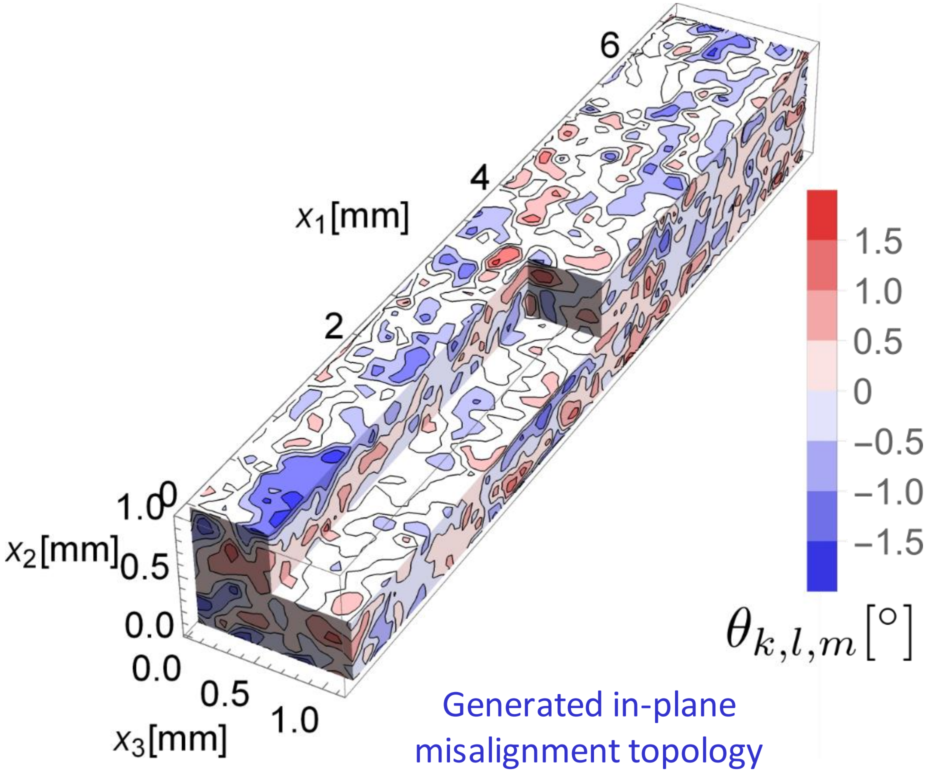

Generated in-plane misalignment topology

Quantification of uncertainty in strength

Numerical modeling for failure probability: Model Geometry

- [Ref. 5]: Homogenized representation of fiber and matrix at micro level with 20 node C3D20 elements
- Misalignments given as local material orientations at element integration points

- PBC in direction 1 and 2, free surfaces in direction 3
- Displacement loads

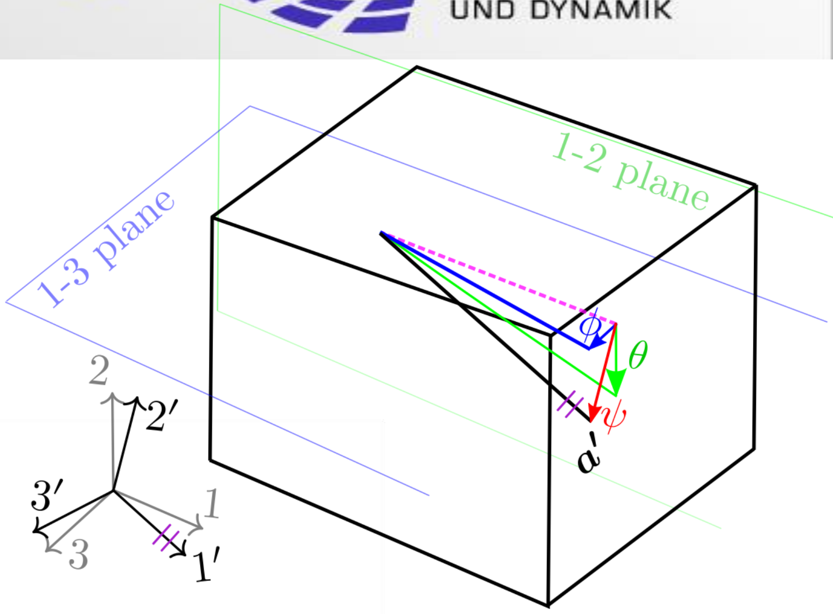

Preferred direction shown in an element

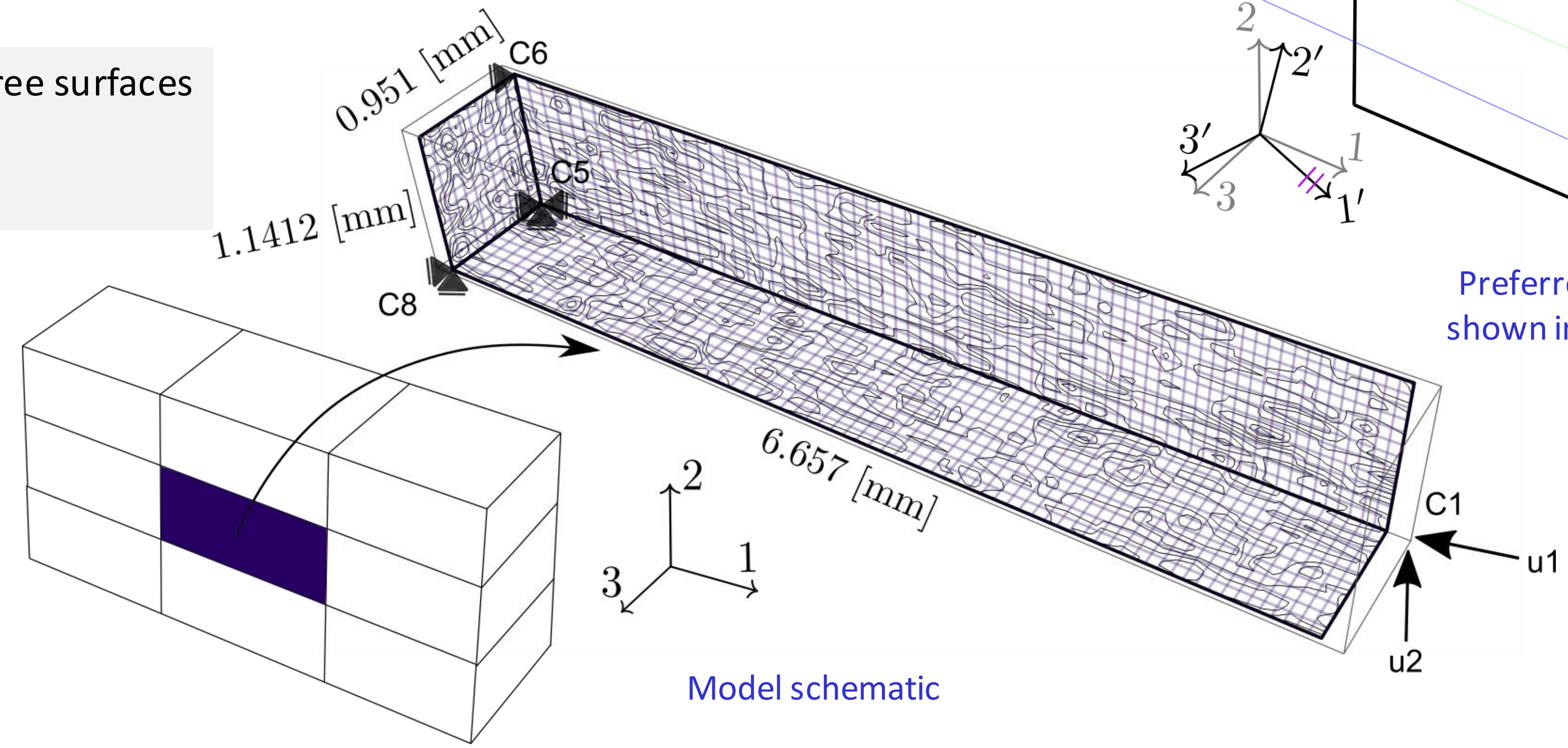

Model schematic

Quantification of uncertainty in strength

Numerical modeling for failure probability: Experimental vs Numerical Approaches

- [Ref. 5]: Comparison using Weibull scaling law
- Close match between median values from experiments and avg model based on scaling law
- Model prediction scatter quite less leading to high m value
- Model size: 6.657x1.1412x0.951 mm
- Specimen size: 5x5x1.15 mm

$$\frac{\sigma^c_{avg-model}}{\sigma^c_{exp}} = \left(\frac{V_{avg-model}}{V_{exp}}\right)^{-1/m}$$

Model	exp	Dotted curve
25.78	7.11	7.75

m parameter

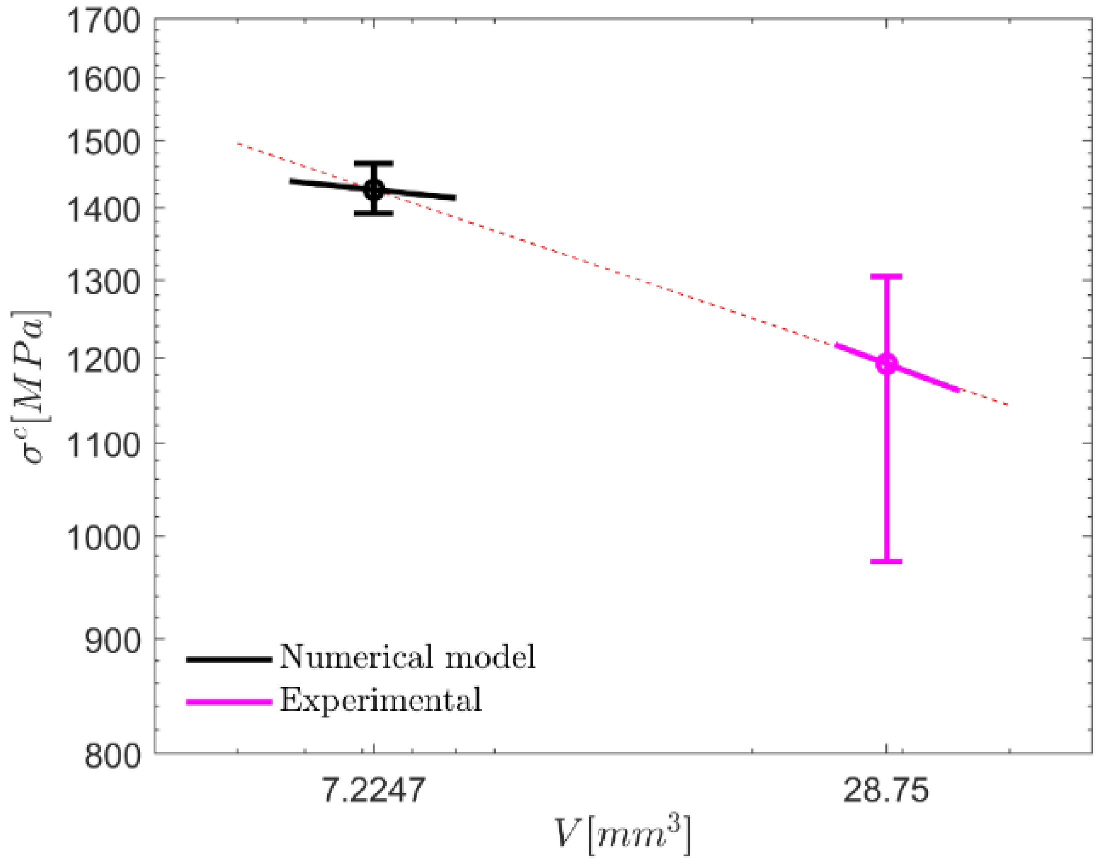

Numerical vs Experimental results

Quantification of uncertainty in strength

Numerical modeling for failure probability: Experimental vs Numerical Approaches

INSTITUT FÜR STATIK UND DYNAMIK

- [Ref. 5]: Numerical failure envelopes valid for a volume of 6.657x1.1412x0.951 mm whereas experimental envelopes valid for 5x5x1.15 mm
- Scale effects on compression part of envelopes visible clearly
- More load cases in numerical models lead to prediction of intricate shapes precisely

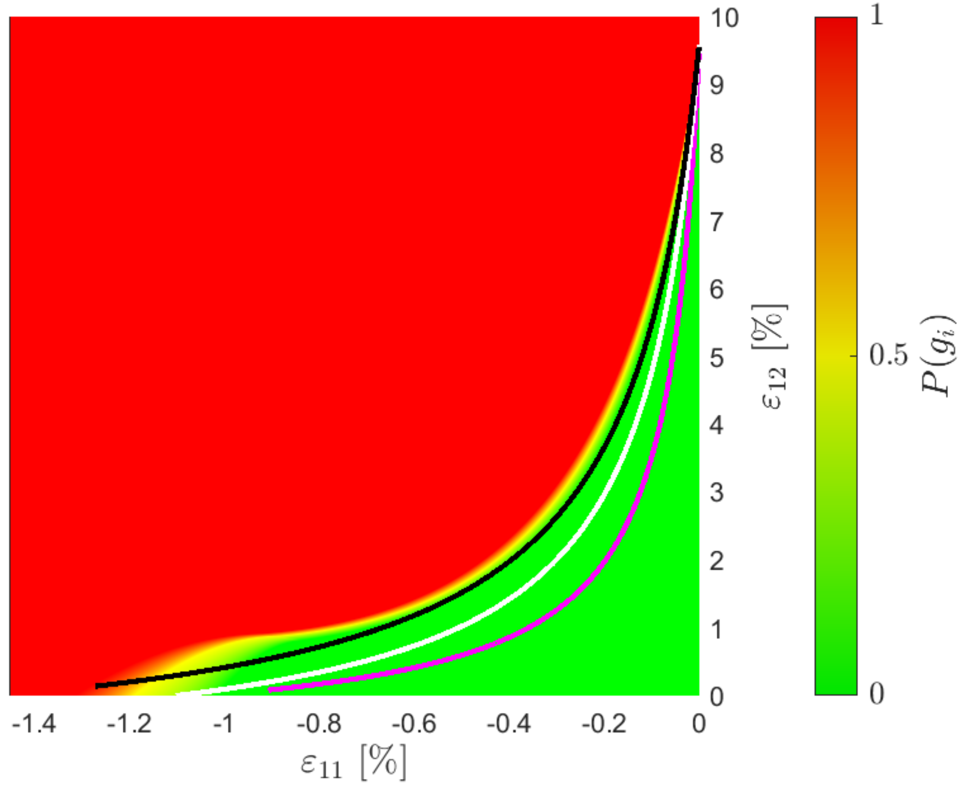

Comparison of failure envelopes in strain space

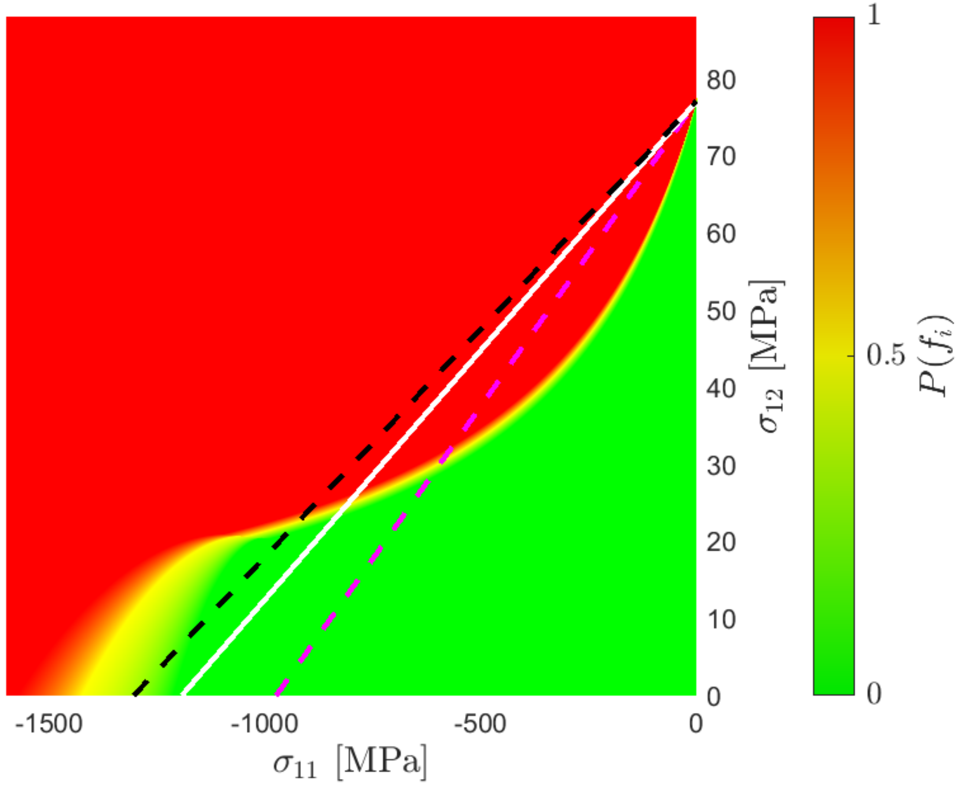

Comparison of failure envelopes in stress space

Quantification of uncertainty in strength

Numerical modeling for failure probability: Size effects in NCF composites

- [Ref. 8]: Misalignment derived from measurements
- Predictions resulting from the weakest-link Weibull theory are compared against strength–size statistics gathered by numerical analysis
- Generally, weakest-link Weibull theory applicable to size effects, however, bonded plies inconsistent with the weakest-link assumption

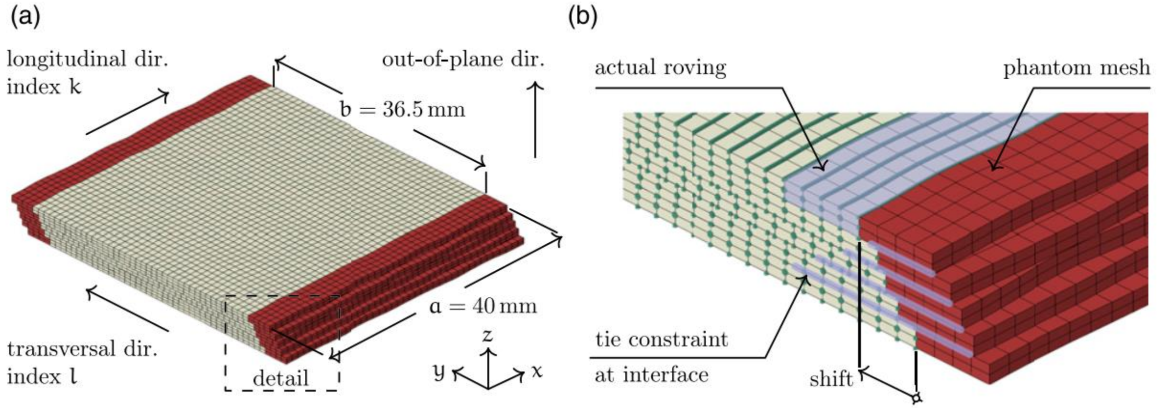

A view of the undeformed mesh of a five ply model
(a) global view, (b) magnified view

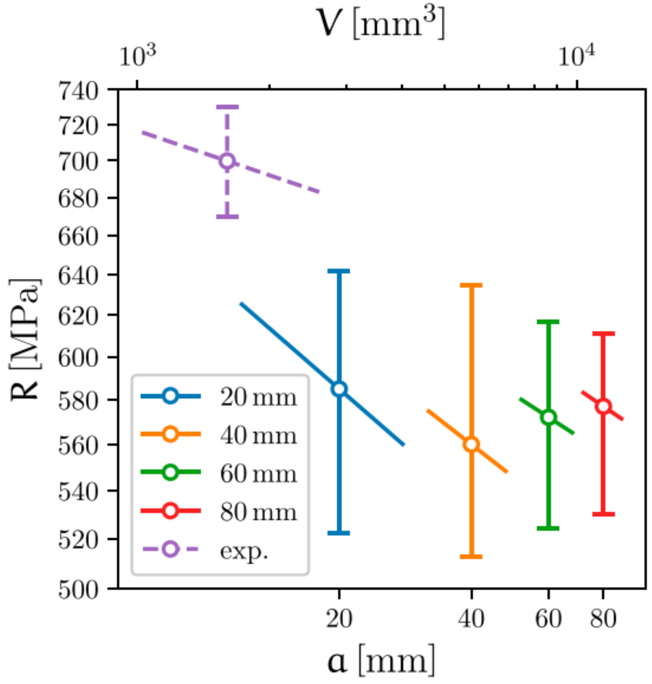

Percentiles of observed strength R over effective volume V

Outlook

- Investigations of scale effects under homogenous compression load through numerical and experimental approaches
- Methodologies for failure initiation and final failure scale laws in components such as holed specimens
- Use of probabilistic failure envelopes in combination with composite laminate theory for defining a safe region
- Use of machine learning algorithms for probabilistic analyses under compression dominated loads …

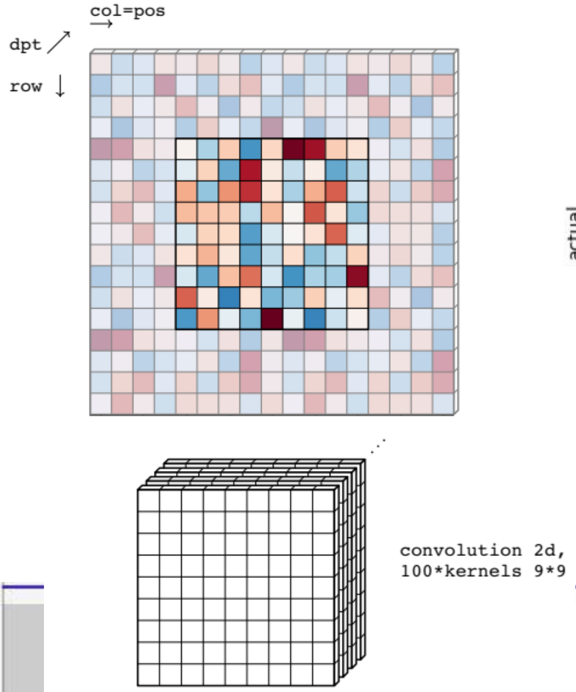

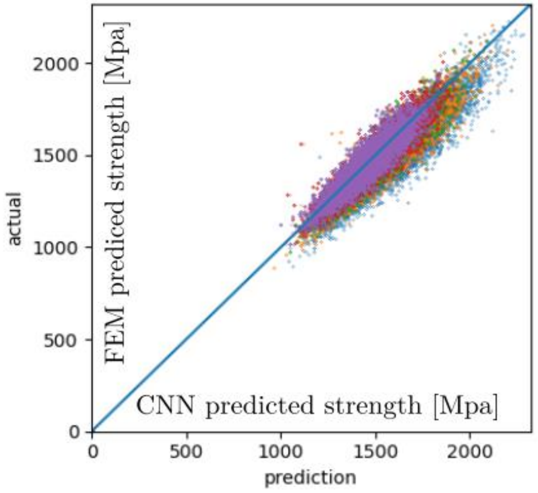

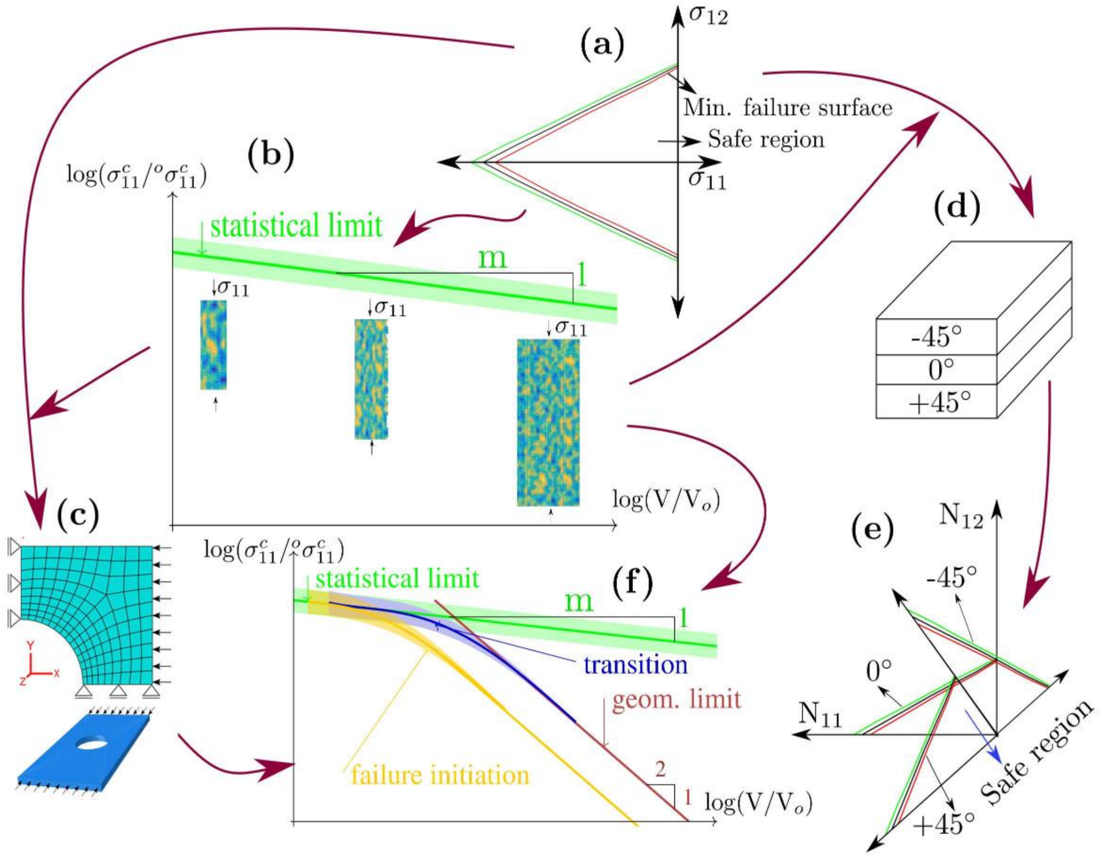

Topics of interest

References

- [1] M. Bishara, R. Rolfes, and O. Allix. “Revealing complex aspects of compressive failure of polymer composites – Part I: Fiber kinking at microscale.” Composite Structures 169.Supplement C 2017.
- [2] M. Bishara, M. Vogler, and R. Rolfes. “Revealing complex aspects of compressive failure of polymer composites – Part II: Failure interactions in multidirectional laminates and validation.” Composite Structures 169.Supplement C 2017.
- [3] B Daum and R Rolfes. “A micropolar approach to microbuckling problems in unidirectionally reinforced polymer composites.” Mechanics of Materials 2021.
- [4] A. Dean, N. Safdar, and R. Rolfes. “A Co-Rotational Based Anisotropic ElastoPlastic Model for Geometrically Non-Linear Analysis of Fibre Reinforced Polymer Composites: Formulation and Finite Element Implementation.” Materials, 2019.
- [5] N. Safdar, B. Daum, and R. Rolfes. “A numerical prediction of failure probability under combined compression-shear loading for unidirectional fiber reinforced composites.” Mechanics of Materials 2022.
- [6] N. Safdar, B. Daum, R. Rolfes. "The effect of model dimensionality on compression strength of fiber reinforced composites." Journal of Composite Materials, 2022.
- [7] N Safdar, B Daum, S Scheffler, and R Rolfes. “Experimental determination of a probabilistic failure envelope for carbon fiber reinforced polymers under combined compression-shear loads.” International Journal of Solids and Structures 2022.
- [8] B. Daum, G. Gottlieb, N. Safdar, M. Brod, J.H. Ohlendorf, and R. Rolfes. “A numerical investigation of the statistical size effect in non-crimp fabric laminates under homogeneous compressive loads.” Journal of Composite Materials, 2021.